Annual forest and evergreen forest cover maps in the Brazilian Amazon in terms of FAO's forest definition

Yuanwei Qin[1], Xiangming Xiao[1*], Hao Tang[2], Ralph Dubayah[3], Russell Doughty[4], Diyou Liu[5], Fang Liu[1], Yosio Shimabukuro[6], Egidio Arai[6], Xinxin Wang[7], Berrien Moore III[4]

5

[1]Department of Microbiology and Plant Biology, University of Oklahoma, Norman, OK 73019, USA

[2]Department of Geography, National University of Singapore, 1 Arts Link, Kent Ridge, Singapore 117570

[3]Department of Geographical Sciences, University of Maryland, College Park, MD, USA

[4]College of Atmospheric and Geographic Sciences, University of Oklahoma, Norman, OK, 73019, USA

10   [5]College of Land Science and Technology, China Agricultural University, Beijing 100083, China

[6]Brazilian National Institute for Space Research, INPE, São José dos Campos, SP, Brazil

[7]Coastal Ecosystems Research Station of the Yangtze River Estuary, Ministry of Education Key Laboratory of Biodiversity Science and Ecological Engineering, Institute of Biodiversity Science, School of Life Sciences, Fudan University, Shanghai 200438, China

15

Correspondence to: Xiangming Xiao (xiangming.xiao@ou.edu)

Abstract. Many forest cover maps have been generated by using optical and/or microwave images and various forest definitions, but these forest cover maps have large discrepancies. Both forest definition and validation data used for accuracy
20   assessment of forest cover maps are often considered as two of the major factors for the discrepancy among these forest cover maps. To date, few studies have assessed forest cover maps in terms of two biophysical parameters used in forest definition: (1) tree canopy height and (2) canopy coverage. We generated annual forest cover maps from 2007 to 2010 and evergreen forest cover maps from 2000 to 2021 in the Brazilian Amazon using the images from the Phased Array type L-band Synthetic Aperture Radar and Moderate Resolution Imaging Spectroradiometer, and the forest definition of the Food and Agriculture
25   Organization (FAO) of the United Nations (>5-m tree height and >10% canopy coverage). The canopy height and coverage datasets from the Geoscience Laser Altimeter System during 2003-2007 were used to assess annual forest cover maps from 2007 to 2010 and evergreen forest cover maps from 2003 to 2007, and the results show high accuracy of these forest and evergreen forest cover maps in the Brazilian Amazon.

30   **1. Introduction**

The global forest area is 40.6×10^6 km^2 and accounts for ~31% of the total land area, according to the 2020 Global Forest Resources Assessment (FRA) published by the Food and Agriculture Organization (FAO) of the United Nations (Fao, 2020). Forests, especially tropical forests, play major roles in the carbon cycle (Fan et al., 2019; Mitchard, 2018), water cycle (Lovejoy and Nobre, 2019), and biodiversity (Jenkins et al., 2013). Tropical forests contain ~230 Pg C aboveground biomass,

35   which is ~40% to ~60% of the carbon stored in Earth's terrestrial vegetation (Baccini et al., 2012; Saatchi et al., 2011). However, large areas of forests have been deforested for agriculture, wood, and charcoal production (Fao, 2020). A total of 1.8×10^6 km^2 of forests have been lost since 1990 due to human activities and natural disturbances, although the rate of net forest loss has declined slightly (Fao, 2020). The extensive forest area loss caused significant losses of forest carbon stock (Mitchard, 2018) and biodiversity (Ochoa-Quintero et al., 2015). Thus, updated and accurate annual maps of forests are

40   essential for people to track and assess the loss and gain of forest area and their impacts on carbon, water, climate, and biodiversity.

        Satellite remote sensing can observe large land surface areas at regular temporal resolutions, which is suitable for generating annual maps of forests at regional, continental, and global scales. Substantial progress has been achieved in identifying and mapping the spatial and temporal changes of forests across local, regional, and global spatial scales by using

45   various image datasets and algorithms (Souza et al., 2020; Fao, 2020; Hansen et al., 2013; Shimada et al., 2014). The time series optical remote sensing images at coarse and moderate spatial resolutions, such as the Advanced Very High Resolution Radiometer (AVHRR, 1000-m) and MODIS (500-m and 250-m), have been widely used to generate global or continental forest cover maps, which were based on forest spectral and phenology features (Friedl et al., 2010; Hansen et al., 2002). Before 2008, optical images at high spatial resolution (e.g., Landsat) were expensive and often used to map forests in the hotspots of

50   deforestation, such as the Brazilian Amazon (Skole and Tucker, 1993; Inpe, 2020). In 2008, all the 30-m Landsat images became freely available to the public (Woodcock et al., 2008). Google Earth Engine, a powerful and free cloud computing platform, was also developed to process these big datasets(Gorelick et al., 2017). Continental or global tree cover and forest cover maps at high spatial resolution have been generated using Landsat images (Sexton et al., 2015; Hansen et al., 2013; Souza et al., 2020).

55   In comparison to the optical images, images from microwave sensors, in particular, L-band synthetic aperture radar (SAR), have two advantages: (1) they are affected less by clouds and cloud shadow, and (2) they are more sensitive to forest structure and biomass. SAR images have advantages in forest mapping, especially in the tropical region where clouds and cloud shadows are frequent (Qin et al., 2017; Shimada et al., 2014; Qin et al., 2016a; Chen et al., 2018; Reiche et al., 2016). In the Advanced Land Observing Satellite (ALOS), the Phased Array type L-band Synthetic Aperture Radar (PALSAR) is the

60   first L-band microwave remote sensing sensor to carry out global land surface observations (Shimada et al., 2014). The 25-m and 50-m ALOS PALSAR data have been used to map regional and global forest and forest change (Shimada et al., 2014; Qin et al., 2017; Chen et al., 2018; Thapa et al., 2014). However, some non-forest land cover types, such as rocky land, bare land, and buildings, have high backscatter signals, similar to those of forests, and they are misclassified as forest, resulting in commission errors in the forest cover maps. The combination of microwave and optical images allows us to produce improved

65   forest cover maps with reduced commission errors. Thus, we developed a simple and robust algorithm to identify and generate annual forest cover maps using both ALOS PALSAR and MODIS images, and the algorithm has been successfully applied to map forest in Asia (Qin et al., 2015; Qin et al., 2016a) and South America(Qin et al., 2017; Qin et al., 2019).

Previous studies suggested that forest definition is one of the major reasons for the discrepancy of forest cover maps (Sexton et al., 2015), and our study showed the validation data affect accuracy assessment of forest cover maps although these

70 forest cover maps had the same forest definition (Qin et al., 2017). Accuracy assessments and uncertainty analyses of the forest cover maps have been carried out using reference datasets from various approaches, including field surveys, images with very high spatial resolutions, and previously available land cover maps(Xiao et al., 2011; Fritz et al., 2012; Olofsson et al., 2012; Stehman et al., 2012; Tyukavina et al., 2017). Field surveys are carried out either over a region or at fixed locations that aim to track long-term forest area and biomass changes under human activities and natural disturbances(Matricardi et al., 2020).

75 These field forest surveys are time-consuming and have a high labor cost, thus, limited field samples are collected, which may introduce large bias and are not suitable to assess the forest cover maps at continental or global scales(Tang et al., 2019a). The very high spatial resolution images and land cover maps do not have accurate canopy height information, which is one of the primary criteria for forest definition.

Tree canopy height and canopy coverage are two important characteristics of forests. Airborne lidar observations are

80 being used to accurately measure canopy height and canopy coverage, but these measurements are mainly carried out at a local scale(Tang et al., 2019b; Hudak et al., 2002; Leitold et al., 2018). The satellite Lidar-based canopy height and canopy coverage monitoring has evolved remarkably, which provides an opportunity to use them to evaluate the accuracy and uncertainty of forest cover maps and improve forest mapping. Recently, new and reliable canopy height and canopy cover percentage datasets(Tang et al., 2019a) were generated using the Geoscience Laser Altimeter System (GLAS) onboard the Ice, Clouds,

85 and Land Elevation Satellite (ICESat) satellite. These new datasets provide a unique opportunity to assess annual forest cover maps generated according to the FAO FRA forest definition (trees > 5-m height and 10% canopy coverage).

Here, we selected the Brazilian Amazon as a hotspot with a large forest area and extensive forest change. We assessed the annual PALSAR/MODIS forest cover maps at 50-m spatial resolution during 2007-2010(Qin et al., 2017) and the MODIS evergreen forest cover maps during 2003-2007 at 500-m spatial resolution (Qin et al., 2019) using the ICESat/GLAS canopy

90 height and canopy coverage data. To our limited knowledge, this is the first study using a large lidar-based canopy height and canopy coverage dataset to assess the accuracy and uncertainty of annual forest cover maps in the Brazilian Amazon.

2. Methods

2.1. Study area

95 The Brazilian Amazon covers an area between 18˚S to 6˚N and 74˚ W to 41˚ W, and includes nine states (Acre, Amazonas, Amapa, Para, Mato Grosso, Maranhao, Rondonia, Roraima, and Tocantins). The Brazilian Amazon has the largest tropical forests and most diverse terrestrial ecosystems in the world(Jenkins et al., 2013). Annual precipitation increases from ~1500 mm per year in the southeast to > 3000 mm per year in the northwest in normal years (Qin et al., 2019). On the average, the Brazilian Amazon has annual precipitation of ~2000 mm per year and annual mean temperature of 27 ˚C (Almeida et al.,

100 2017). The two major biomes in Brazil are the Amazon evergreen forests in the north and west, and the Cerrado, *i.e.*, a vast ecoregion of tropical savanna, in the south and east. Rapidly changing land use, disturbances (e.g., fire), climate, and other

human activities have resulted in substantial deforestation and degradation in the Brazilian Amazon over the past decades(Fearnside, 2005; Nepstad et al., 2014; Matricardi et al., 2020). The rapid expansion of cropland and pasture areas makes Brazil a leading global exporter of agricultural and livestock commodities, especially soybean and beef.

2.2. ALOS PALSAR mosaic data and pre-processing

The ALOS PALSAR is an L-band active microwave remote sensing sensor, and PALSAR images are less affected by cloud and atmospheric conditions than optical images. The 50-m ALOS PALSAR mosaic data, provided by the Earth Observation Research Center, JAXA, include HH gamma-naught and HV gamma-naught, and three other layers (mask information, local incidence angle, and total dates from the ALOS launch date)(Shimada et al., 2014). Three major pre-processing tasks were carried out to reduce the noise in the ALOS PALSAR data (Shimada et al., 2014). The ALOS PALSAR strip data, with the minimum response to surface moisture, were used to generate the annual ALOS PALSAR mosaic data. The raw images were calibrated based on published coefficients, and outputs with 16-looks were provided to reduce speckle noise further. PALSAR HH and HV backscatter data were orthorectified, and slope corrected using the Digital Elevation Model (90-m) from the Shuttle Radar Topography Mission. The Digital Number (DN) (amplitude values) of HH and HV were converted to backscattering coefficients in decibels (gamma-naught, γ°) (see Equation 1).

$$\gamma^{\circ} = 10 \times log_{10} < DN^2 > + CF \quad (1)$$

Where CF is the absolute calibration factor with a value of -83(Shimada et al., 2009). We also calculated the Difference (see Equation 2) and Ratio (see Equation 3) between HH and HV:

$$Difference = HH - HV \quad (2)$$

$$Ratio = {HH}/{HV} \quad (3)$$

2.3. MODIS surface reflectance and vegetation indices

The MOD09A1 data product provides land surface reflectance after atmospheric correction, including gases, aerosols, and Rayleigh scattering. The MOD09A1 data product has seven spectral bands: Blue (459 - 479 nm), Green (545 - 565 nm), Red (620 - 670 nm), Near-Infrared (NIR, 841 - 876 nm), NIR (1230 - 1250 nm), Shortwave Infrared (SWIR, 1628 - 1652 nm, and 2105 - 2155 nm), and two quality layers. For each 8-day composite, the best-quality value is selected from all the acquisitions within every eight days. We identified and excluded all observations in each image covered by cloud (cloud, internal cloud, and high cirrus), cloud shadow, high aerosols, or snow labelled in the data quality layers. We also identified and excluded all the observations with a blue band value larger than 0.2 as an additional cloud flag. We then calculated three vegetation indices for each observation in time series (see Equation 4, 5, 6): Normalized Difference Vegetation Index (NDVI), Enhanced Vegetation Index (EVI), and Land Surface Water Index (LSWI)(Xiao et al., 2002).

$$NDVI = \frac{NIR - RED}{NIR + RED} \quad (4)$$

$$EVI = 2.5 \times \frac{NIR - RED}{NIR + 6 \times RED - 7.5 \times BLUE + 1} \quad (5)$$

$$LSWI = \frac{NIR - SWIR}{NIR + SWIR} \quad (6)$$

where BLUE, RED, NIR and SWIR represent land surface reflectance values for blue, red, near infrared (841 – 875 nm), and shortwave infrared (1628 – 1652 nm) bands from MOD09A1, respectively.

The MODIS/Terra Vegetation Index data product (MOD13Q1) has a spatial resolution of 250-m and a temporal resolution of 16 days. The MOD13Q1 dataset includes two vegetation index layers (NDVI and EVI). The highest NDVI and EVI values were chosen from the best available observations every 16 days. We exclude the bad-quality observations and only use good-quality observations in time series analysis based on the pixel quality layers. In this study, we used the NDVI layer and calculated the maximum NDVI values (NDVImax) in a year for each pixel during 2007-2010.

2.4. ICESat canopy height and cover percentage data

The ICESat GLAS, launched in 2003, is the first lidar sensor for global land surface observations. The GLAS sensor recorded the land surface elevations through time at ~65-m footprints, which have an along-track distance of about 175 m and a maximum between-track distance of about 30 km at the equator. We recently developed a new approach and calculated the canopy height (meters) and canopy coverage (%) datasets using the GLA14 lidar datasets during 2003-2007(Tang et al., 2019a). At each footprint, maximum canopy height and canopy coverage are calculated from lidar waveform signals and screened from several confounding factors (e.g., cloud, noise, and topographic slope)(Tang et al., 2019a). The derived canopy coverage showed almost no bias compared to airborne lidar estimates and was sensitive to signal dynamics over dense forests, even with canopy cover exceeding 80%. The ICESat/GLAS-based canopy height and canopy coverage estimates could better characterize footprint-level canopy conditions than the existing data products derived from conventional optical remote sensing(Tang et al., 2019a). Yet, it cannot be used to generate a wall-to-wall map of forest structure due to its limited spatial samplings.

In the Brazilian Amazon, there were about 1.1 million footprints of canopy height and canopy coverage retrieved from the ICESat/GLAS observations during 2003-2007 (Fig. 1). Among these footprints, about 1.0×10^6 footprints had a canopy height of more than 5 meters, which accounted for about 96% of all the footprints (Fig. 1c), and about 0.94×10^6 (86.7%) of the footprints had canopy coverage of more than 10% (Fig. 1d). When considering both canopy height and canopy coverage, 0.9×10^6 footprints (85.1%) had canopy height of > 5 meters and canopy coverage of > 10%, which were thus identified as forest footprints in terms of the FAO FRA forest definition. About 27.7% of the forest footprints had canopy height larger than 30 meters and canopy coverage larger than 80%, which suggested that the Brazilian Amazon is an area with largely tall and dense trees. The ICESat/GLAS canopy height and coverage data had distinct spatial distributions (Fig. 1a, b). Those tall and dense forests were mainly located north and west of the Brazilian Amazon, where human activities and natural disturbances are limited. Short and open forests were mainly located in the Cerrado area south and east of the Brazilian Amazon, where extensive agriculture production occurs.
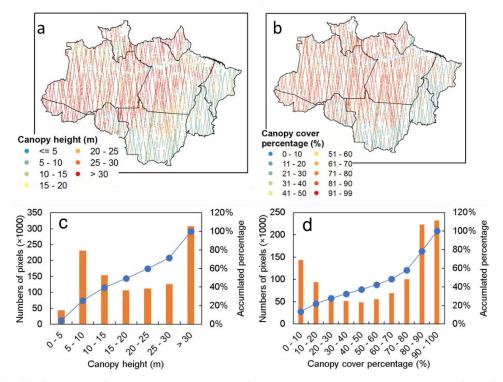
Fig. 1. Spatial distribution maps of ICESat-GLAS canopy height (a) and canopy coverage (b) at the footprint scale and their histograms (c-d) in the Brazilian Amazon.

2.5. FAO forest definition

Hundreds of different forest definitions have been used in forest management (Unfao, 2002; Lund, 2014). FAO defines forest as land with a minimum area of 0.5 hectares with (1) a tree canopy height of > 5 meters and (2) a canopy coverage of >10% at the time of observations, and it also includes lands with trees that can reach these thresholds at the time of tree mature(Fra, 2020). Using the FAO's forest definition, we identified and generated two sets of annual forest cover maps in the Brazilian Amazon during 2000-2021, including annual PALSAR/MODIS forest maps from 2007 to 2010 and annual evergreen forest maps from 2000 to 2021. Note that as we use satellite images to identify and map forests, we do not consider lands with trees that can reach these two thresholds at the time of tree mature.

2.6. Annual PALSAR/MODIS forest cover maps during 2007-2010

Using the FAO's forest definition, we developed a robust workflow to identify and generate forest cover maps by integrating ALOS PALSAR and MODIS NDVImax data(Qin et al., 2016a; Qin et al., 2015; Qin et al., 2017). PALSAR data can penetrate the tree canopy and interact with the tree trunks and branches. Forests have higher volume backscatter signals in HH and HV compared to croplands, grasslands, and water bodies. Thus, PALSAR data are sensitive to forest structure and biomass. However, PALSAR data can be affected by local incidence angle and soil moisture as PALSAR data is acquired at

6

a different date each year. We calculated the acquisition date (Fig. 2), the local incidence angle (Fig. 3), and HH and HV gamma-naught values for each year and their standard deviations (Fig. 4) during 2007-2010 in the Brazilian Amazon. PALSAR HH and HV data were mainly acquired in the dry season and the local incidence angle is stable. About 90% of the area has
185 standard deviation values of less than 1 dB for PALSAR HH and HV data. Therefore, PALSAR data have advantages in identifying and mapping the spatial and temporal changes of forests in the tropics with frequent clouds compared to optical satellite remote sensing. Several land cover types (e.g., rocks and buildings) have high backscatter values of HH and HV, which are often confused with the forests when only HH and HV data are used. To reduce the commission errors from these land cover types, we used both PALSAR and NDVImax from MOD13Q1 to produce annual maps of forests (namely
190 PALSAR/MODIS) at 50-m spatial resolution in the Brazilian Amazon during 2007-2010 using these threshold values: $-15 \leq$ HV ≤ -9, $3 \leq$ Difference ≤ 7, $0.35 \leq$ Ratio ≤ 0.75, and NDVImax ≥ 0.5 (Qin et al., 2016a; Qin et al., 2017). We also carried out a three-year temporal consistency filter to reduce the effects of noise (Qin et al., 2016a; Qin et al., 2017).
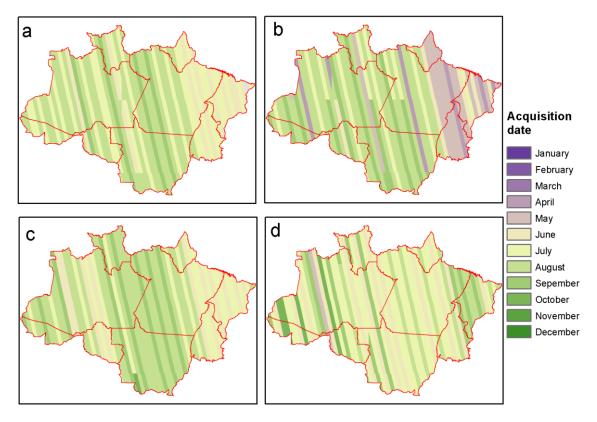

Fig. 2. Spatial distribution maps of ALOS PALSAR acquisition date during 2007-2010. (a) 2007. (b) 2008. (c) 2009. (d) 2010.
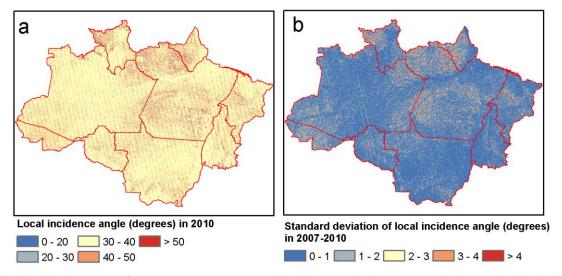
Fig. 3. Spatial distribution maps of ALOS PALSAR data local incidence angle in 2010 (a) and the standard deviation of local incidence angle from 2007 to 2010 (b).
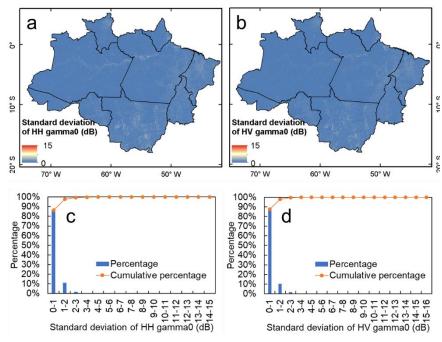

Fig. 4. Spatial distribution maps of the standard deviation of PALSAR HH and HV gamma0 (a-b) and their histograms (c-d) during 2007-2010.

Earth System
Science
Data
Open Access
Discussions

2.7. Annual MODIS evergreen forest cover maps during 2000-2021

Evergreen forest is the dominant forest cover type in the Brazilian Amazon (Fanin and Van Der Werf, 2015).

205 Evergreen forests have a unique biophysical feature that evergreen forests have green leaves year-round. Based on the canopy phenology from analyses of time series water-related LSWI and greenness-related EVI calculated from MOD09A1 product, a novel, simple and robust algorithm was developed to generate annual maps of evergreen forests in the tropical zone using the FAO's forest definition (Xiao et al., 2009; Qin et al., 2019). We calculated (1) the frequency (percentage) of the number of observations with LSWI ≥ 0 over all the good observations ($FQ_{LSWI≥0}$) and (2) the minimum EVI values (EVI_{min}) in a year

210 after excluding bad-quality observations. We applied the Forest-MODIS algorithm ($FQ_{LSWI≥0} = 100\%$ & $EVI_{min} ≥ 0.2$) (Xiao et al., 2009; Qin et al., 2019) to time series LSWI and EVI data in a year and generated annual maps of evergreen forest from 2000 to 2021 in the Brazilian Amazon. Small numbers of MODIS pixels in the Brazilian Amazon were contaminated by clouds or aerosols, causing a significant drop in EVI values and no significant change in LSWI and NDVI values. However, these pixels may not be detected by the quality layer. Thus, we included an additional criterion and made a minor improvement in

215 evergreen forest mapping, *i.e.*, $FQ_{LSWI≥0} > 90\%$ & $EVI_{min} ≥ 0.2$ & $LSWI_{min} ≥ 0$. We also applied a three-year temporal consistency filter to reduce the effects of noises on forest mapping. The Google Earth Engine (GEE) cloud platform was used for MODIS image processing.

2.8. Spatial and statistical analysis

We overlaid all the ICESat/GLAS footprints to the annual PALSAR/MODIS forest cover maps during 2007-2010

220 (50-m spatial resolution) and the annual MODIS evergreen forest cover maps during 2003-2005 (500-m spatial resolution) and generated a table that records individual ICESat/GLAS footprint IDs, canopy height, canopy coverage, forest and non-forest from the annual forest cover maps. We evaluated the accuracy of these annual forest cover maps in terms of canopy height and canopy coverage for all forest pixels (1.5 billion pixels for PALSAR/MODIS forest and 17.5 million pixels for evergreen forest each year) that have ICESat/GLAS footprint data.

225 For the spatial comparison, we aggregated the 50-m annual PALSAR/MODIS forest cover maps and 500-m MODIS evergreen forest cover maps into 5-km pixels and calculated their average forest area fraction values within individual 5-km pixels. We then compared the spatial consistency between the annual PALSAR/MODIS forest cover maps and the annual MODIS evergreen forest cover maps in 2007-2010 in the Brazilian Amazon at 5-km spatial resolution.
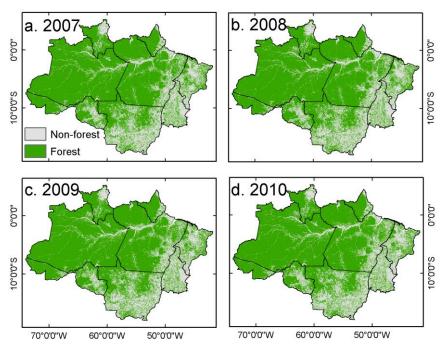
230 **3. Results and Discussions**

3.1. Annual PALSAR/MODIS forest cover maps in 2007-2010

Forest areas estimated by the 50-m PALSAR/MODIS forest cover maps (Fig. 5) had a small net loss in the Brazilian Amazon, decreasing from $3.77 × 10^6$ km² in 2007 to $3.75 × 10^6$ km² in 2010 under the influence of changing land-use policies and natural disturbances(Nepstad et al., 2014). Using 18 $5 × 5$ km² blocks ($0.15 × 10^6$ pixels) of land cover maps at 2-m spatial

235 resolution from the Global Land Cover Validation Reference Dataset in 2010(Olofsson et al., 2012; Stehman et al., 2012) and 416 10×10 km² blocks ($17.09 × 10^6$ pixels) of land cover maps from the TREES-3(Achard et al., 2014) reference dataset at

30-m spatial resolution from the European Commission's Joint Research Centre (JRC), the overall accuracy of the PALSAR/MODIS forest cover map in 2010 was about 91%(Qin et al., 2019).

Fig. 5. Spatial distribution maps of annual PALSAR/MODIS forest cover maps in 2007-2010. (a) 2007. (b) 2008. (c) 2009. (d) 2010.

We used the ICESat/GLAS canopy height and canopy coverage to evaluate the accuracy of annual PALSAR/MODIS forest cover maps during 2007-2010 in the Brazilian Amazon. Fig. 6 shows the distribution of forest pixels from the annual PALSAR/MODIS forest cover maps in the 2-dimension space of canopy height and canopy coverage. About 98.5% of PALSAR/MODIS forest pixels in 2010 had canopy height > 5 meters and about 94.4% of PALSAR/MODIS forest pixels in 2010 had canopy coverage > 10%, respectively (Fig. 6). When considering both canopy height and canopy coverage, about 93.8% (0.75×10^6 pixels) of PALSAR/MODIS forest pixels in 2010 had both canopy height of > 5 meters and canopy coverage of > 10%, consistent with the FAO forest definition. The PALSAR/MODIS forest cover maps in 2007-2009 had similar high accuracies as in 2010 (Fig. 6). Overall, the PALSAR/MODIS forest cover maps showed high accuracies using different validation datasets.
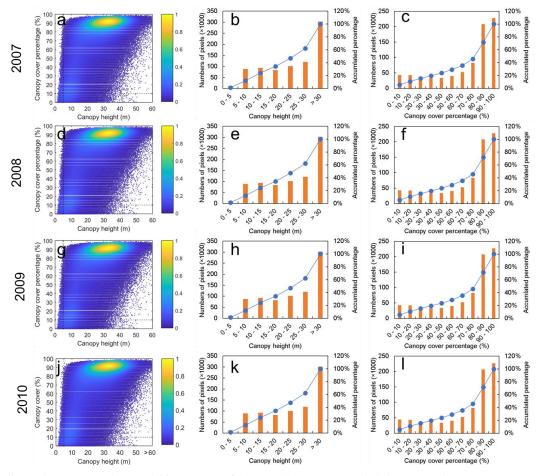
Fig. 6. Two-dimension scatter plots and histograms of ICESat/GLAS canopy height (m) and canopy coverage (%) at the footprint scale for the forest pixels in the annual PALSAR/MODIS forest cover maps during 2007-2010.

255

Geographically, forests were distributed mainly in the Brazilian Amazon's north and west. The mixed landscapes of forest and non-forest were in the south and east of the Brazilian Amazon (Fig. 5). The State of Amazonas (1.46×10^6 km²), Pará (0.99×10^6 km²), and Mato Grosso (0.46×10^6 km²) had the largest forest areas, which accounted for about 78% of the total forest area in the Brazilian Amazon in 2010. The other six states had a total forest area of 0.81×10^6 km² in 2010.

260 **3.2. Annual MODIS evergreen forest cover maps in 2000-2021**

Evergreen forest areas also slightly decreased from 3.73×10^6 km² in 2007 to 3.72×10^6 km² in 2010 in the Brazilian Amazon (Fig. 7), consistent with the PALSAR/MODIS forest area estimates with a Root Mean Square Error (RMSE) of 0.03×10^6 km². The evergreen forest area was 3.94×10^6 km² in 2000 and then declined substantially to 3.66×10^6 km² in 2021 (Fig. 7), with a net forest area loss of 0.28×10^6 km² (7%). We previously assessed the accuracy of the evergreen forest cover map in 2010 using 18 5×5 km² blocks (1,268 pixels) of land cover maps at 2-m spatial resolution from the Global Land Cover

265

Validation Reference Dataset in 2010 and 416 10×10 km^2 blocks (131,418 pixels) of land cover maps from the 30-m TREES-3(Achard et al., 2014) reference dataset. The overall accuracy of the MODIS evergreen forest cover map in 2010 was about 97%(Qin et al., 2019).
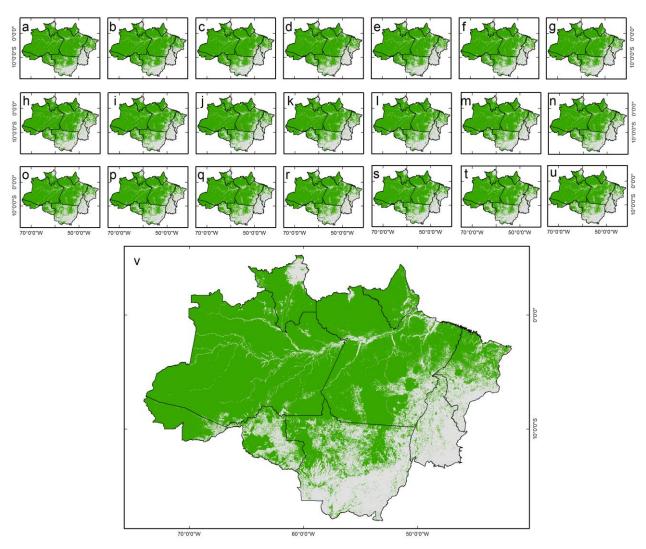

Fig. 7. Spatial distribution maps of annual MODIS evergreen forest cover maps in the Brazilian Amazon during 2000-2021. (a-u) Annual evergreen forest cover maps from 2000 to 2020. (v) Annual evergreen forest cover map in 2021.

Here, we used the ICESat/GLAS canopy height and canopy coverage data to evaluate the accuracy of the evergreen forest cover maps during 2003-2007 in the Brazilian Amazon. About 98.1% (0.77×10^6 pixels) of evergreen forest pixels had canopy height of > 5 meters, and about 93.8% (0.73×10^6 pixels) of evergreen forest pixels had canopy coverage of > 10% in 2003-2007. When considering both canopy height and canopy coverage, about 93.0% (0.73×10^6 pixels) of evergreen forest

pixels in 2003-2007 had canopy height of > 5 meters and canopy coverage of >10%, consistent with the FAO forest definition (Fig. 8).
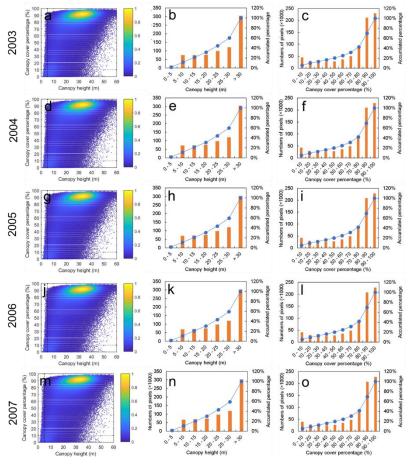

Fig. 8. Two-dimension scatter plots and histograms of ICESat/GLAS canopy height and coverage for the forest pixels from the annual MODIS evergreen forest maps during 2003-2007.

3.3. Spatial consistency between annual PALSAR/MODIS forest cover maps and annual MODIS evergreen forest cover maps in 2007-2010

At the regional scale, we then analysed the reasonability of the MODIS evergreen forest cover maps in the Brazilian Amazon using the PALSAR/MODIS forest maps as the reference maps. At the 5-km spatial resolution, the annual PALSAR/MODIS forest cover maps had good spatial consistency with evergreen forest cover maps, especially in the dense forest during 2007-2010 (Fig. 9). The PALSAR/MODIS forest cover maps had more forest area than MODIS evergreen forest cover maps in the Cerrado area in the south and east of the Brazilian Amazon. There might be some non-evergreen forest and sparse forest in the Cerrado, which are not identified as forest in the MODIS evergreen forest cover maps. Overall, the forest

area fraction between the PALSAR/MODIS forest cover maps and the MODIS evergreen forest cover maps was near the 1:1 linear relationship at 5-km spatial resolution (Fig. 9 i-l).
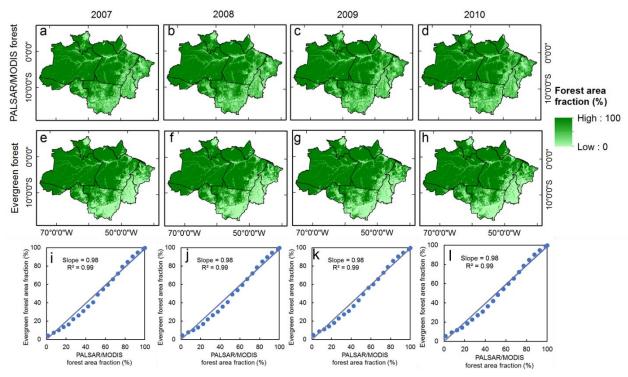

Fig. 9. Spatial consistency between annual PALSAR/MODIS forest cover maps and annual MODIS evergreen forest cover maps during 2007-2010 at a spatial resolution of 5 km. (a-d) Annual PALSAR/MODIS forest cover maps. (e-h) Annual MODIS evergreen forest cover maps. (i-l) Linear regression analyses between the area fraction of MODIS evergreen forest and area fraction of PALSAR/MODIS forest for individual years (2007-2010) at a spatial resolution of 5 km (0.23 million pixels each year). The average area fraction of forest was calculated at an interval of 5%.

3.4. Advantages of using satellite lidar data to assess annual forest cover maps

The recently developed ICESat/GLAS canopy height and canopy coverage dataset has four features(Tang et al., 2019a). First, at the footprint level, the ICESat/GLAS canopy coverage is consistent with the airborne LiDAR estimates with almost no bias. Second, ICESat/GLAS showed higher sensitivity to high coverage in densely forested areas than optical remote sensing images. Third, ICESat/GLAS showed a stronger ability to differentiate subtle temporal changes in canopy coverage compared to optical remote sensing. Fourth, ICESat/GLAS provides unique information about the vertical canopy cover and structure, an important variable in defining tree canopy height.

Tropical forests in the Brazilian Amazon are influenced by mining, deforestation, fires, severe droughts, wind storms, and other disturbances(Tyukavina et al., 2017; Espírito-Santo et al., 2014; Aragão et al., 2018; Sonter et al., 2017; Li et al.,

310   2019). Because of frequent clouds, cloud shadows, high aerosols, and limited accessibility of the Amazon, in situ reference data, field surveys, and very high spatial resolution images are very limited, which prevents a robust inter-comparison among these data sources. The ICESat/GLAS canopy coverage and canopy height datasets have three advantages: (1) sample sizes are very large (e.g., 1.1 million footprints in this study), (2) spatial coverage is extensive, and (3) it provides information on biophysical and structural parameters of forests. In the future, two recently launched platforms, the ICESat-2 satellite launched

315   on September 15, 2018(Markus et al., 2017) and the Global Ecosystem Dynamics Investigation (GEDI) instrument housed on the International Space Station(Dubayah et al., 2020), are providing data that can substantially improve forest cover maps by providing LiDAR-based canopy height and canopy coverage data to the public.

3.5. Annual forest area comparison in the Brazilian Amazon

A number of studies compared several forest cover maps derived from optical images and/or microwave images and

320   reported that these forest cover maps have significant differences in forest area, spatial distributions, and temporal changes, which were attributed to the differences in forest definitions, satellite data, and forest mapping algorithms(Sexton et al., 2015; Qin et al., 2017). For example, one study compared eight previous satellite-based forest cover maps generated by optical images and found that global forest area ranged from 32.1×10^6 km^2 to 41.4×10^6 km^2, and claimed that one of the major reasons underlying the large discrepancy was the ambiguity in the term "forest"(Sexton et al., 2015). Frequent clouds and

325   cloud shadow substantially reduce the number of good-quality observations in optical images used to generate annual forest cover maps in the Brazilian Amazon(Qin et al., 2019). Our previous studies in Asia(Qin et al., 2015; Qin et al., 2016b) and South America(Qin et al., 2017) compared annual forest maps derived from (1) optical images only, (2) microwave images only, and (3) optical + microwave images, and concluded that the use of both optical and microwave images would substantially improve the accuracy of forest maps.

330   Our results here also show that forest area estimates in the Brazilian Amazon from the annual PALSAR/MODIS forest cover maps are consistent with those from the annual MODIS evergreen forest cover maps and the annual PALSAR-based forest cover maps developed by JAXA(Shimada et al., 2014) with both RMSE values of 0.03×10^6 km^2 during 2007-2010 (Fig. 10). Forest area estimates from annual PALSAR/MODIS maps and annual MODIS evergreen forest cover maps are slightly smaller (0.3×10^6 km^2) than that from the Landsat-based Global Forest Watch (GFW) dataset(Hansen et al., 2013)

335   generated using multiple-year Landsat 7 images around 2010. The forest area estimates from the PRODES project(Inpe, 2020) are much smaller than the area estimates by GFW, PALSAR/MODIS, and MODIS evergreen forest cover maps, as the PRODES project is focused on primary forests and deforestation in primary forest areas. Only one or two Landsat-like images that were as cloud-free as possible in the dry season were used to generate annual PRODES forest cover maps(Inpe, 2020). Because of large areas of cloud coverage, annual estimates of forest areas from the PRODES showed large interannual

340   variation(Qin et al., 2019). Our work again demonstrates the importance and potential of L-band microwave remote sensing and daily optical remote sensing images in forest mapping.
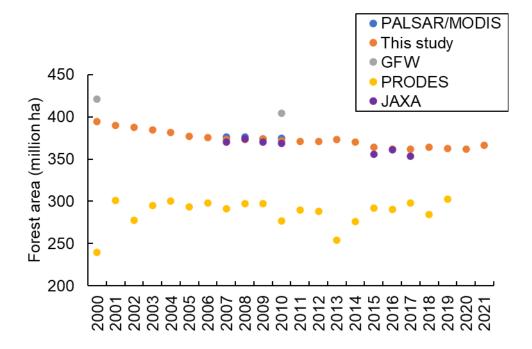
Fig. 10. Annual forest area estimates in the Brazilian Amazon during 2000-2021 from five forest data products.

4. Code and Availability

The annual forest and evergreen forest maps codes are available at the figshare (https://doi.org/10.6084/m9.figshare.21445626) (Qin and Xiao, 2022b). The annual forest maps (2007-2010) and evergreen forest maps (2000-2021) in the Brazilian Amazon have been submitted to the figshare data repository (https://doi.org/10.6084/m9.figshare.21445590) (Qin and Xiao, 2022a) in a GeoTIFF format. The data are provided in the spatial reference of South_America_Albers_Equal_Area_Conic.

5. Conclusion

Accurate forest cover maps are critical for tracking rapid forest changes and forest resource management. We generated annual PALSAR/MODIS forest cover maps and annual evergreen forest cover maps in the Brazilian Amazon from 2000 to 2021 according to the FAO's forest definition. We then assessed the accuracy of the PALSAR/MODIS forest cover maps and evergreen forest cover maps using 1.1 million footprints of canopy height and canopy coverage datasets from ICESat/GLAS. We also compared the reasonability of the evergreen forest maps using the PALSAR/MODIS forest cover maps, which are little affected by the frequent clouds. The accurate PALSAR/MODIS forest cover maps and the evergreen forest cover maps could be used to understand better the interactions between forest and human activities and natural disturbances (Qin et al., 2019; Qin et al., 2021), which is vital to the forest resource management and forest conservation in the Brazilian Amazon.

Author contributions: X.X. and Y.Q. designed the study. Y.Q. and X.X. analysed the data, interpreted the results, and drafted the manuscript. H.T. and R.D. provided the ICESat canopy height and coverage data. All authors reviewed and edited the manuscript.

Competing interests: The authors declare no competing interests.

References

FAO: Global Forest Resources Assessment 2020: Main report. Rome., https://doi.org/10.4060/ca9825en, 2020.

Achard, F., Beuchle, R., Mayaux, P., Stibig, H. J., Bodart, C., Brink, A., Carboni, S., Desclee, B., Donnay, F., Eva, H. D., Lupi, A., Rasi, R., Seliger, R., and Simonetti, D.: Determination of tropical deforestation rates and related carbon losses from 1990 to 2010, Global Change Biol, 20, 2540-2554, 10.1111/gcb.12605, 2014.

Almeida, C. T., Oliveira-Júnior, J. F., Delgado, R. C., Cubo, P., and Ramos, M. C.: Spatiotemporal rainfall and temperature trends throughout the Brazilian Legal Amazon, 1973–2013, Int J Climatol, 37, 2013-2026, https://doi.org/10.1002/joc.4831, 2017.

Aragão, L. E. O. C., Anderson, L. O., Fonseca, M. G., Rosan, T. M., Vedovato, L. B., Wagner, F. H., Silva, C. V. J., Silva Junior, C. H. L., Arai, E., Aguiar, A. P., Barlow, J., Berenguer, E., Deeter, M. N., Domingues, L. G., Gatti, L., Gloor, M., Malhi, Y., Marengo, J. A., Miller, J. B., Phillips, O. L., and Saatchi, S.: 21st Century drought-related fires counteract the decline of Amazon deforestation carbon emissions, Nature Communications, 9, 536, 10.1038/s41467-017-02771-y, 2018.

Baccini, A., Goetz, S. J., Walker, W. S., Laporte, N. T., Sun, M., Sulla-Menashe, D., Hackler, J., Beck, P. S. A., Dubayah, R., Friedl, M. A., Samanta, S., and Houghton, R. A.: Estimated carbon dioxide emissions from tropical deforestation improved by carbon-density maps, Nat Clim Change, 2, 182-185, 10.1038/Nclimate1354, 2012.

Chen, B. Q., Xiao, X. M., Ye, H. C., Ma, J., Doughty, R., Li, X. P., Zhao, B., Wu, Z. X., Sun, R., Dong, J. W., Qin, Y. W., and Xie, G. S.: Mapping Forest and Their Spatial-Temporal Changes From 2007 to 2015 in Tropical Hainan Island by Integrating ALOS/ALOS-2 L-Band SAR and Landsat Optical Images, Ieee J-Stars, 11, 852-867, 10.1109/jstars.2018.2795595, 2018.

Dubayah, R., Blair, J. B., Goetz, S., Fatoyinbo, L., Hansen, M., Healey, S., Hofton, M., Hurtt, G., Kellner, J., Luthcke, S., Armston, J., Tang, H., Duncanson, L., Hancock, S., Jantz, P., Marselis, S., Patterson, P. L., Qi, W., and Silva, C.: The Global Ecosystem Dynamics Investigation: High-resolution laser ranging of the Earth's forests and topography, Science of Remote Sensing, 1, 100002, https://doi.org/10.1016/j.srs.2020.100002, 2020.

Espírito-Santo, F. D. B., Gloor, M., Keller, M., Malhi, Y., Saatchi, S., Nelson, B., Junior, R. C. O., Pereira, C., Lloyd, J., Frolking, S., Palace, M., Shimabukuro, Y. E., Duarte, V., Mendoza, A. M., López-González, G., Baker, T. R., Feldpausch, T. R., Brienen, R. J. W., Asner, G. P., Boyd, D. S., and Phillips, O. L.: Size and frequency of natural forest disturbances and the Amazon forest carbon balance, Nature Communications, 5, 3434, 10.1038/ncomms4434https://www.nature.com/articles/ncomms4434#supplementary-information, 2014.

Fan, L., Wigneron, J. P., Ciais, P., Chave, J., Brandt, M., Fensholt, R., Saatchi, S. S., Bastos, A., Al-Yaari, A., Hufkens, K., Qin, Y., Xiao, X., Chen, C., Myneni, R. B., Fernandez-Moran, R., Mialon, A., Rodriguez-Fernandez, N. J., Kerr, Y., Tian, F., and Penuelas, J.: Satellite-observed pantropical carbon dynamics, Nat Plants, 5, 944-951, 10.1038/s41477-019-0478-9, 2019.

Fanin, T. and van der Werf, G. R.: Relationships between burned area, forest cover loss, and land cover change in the Brazilian Amazon based on satellite data, Biogeosciences, 12, 6033-6043, 10.5194/bg-12-6033-2015, 2015.

Fearnside, P. M.: Deforestation in Brazilian Amazonia: History, rates, and consequences, Conserv Biol, 19, 680-688, DOI 10.1111/j.1523-1739.2005.00697.x, 2005.

FRA: Terms and Definitions, 2020.

Friedl, M. A., Sulla-Menashe, D., Tan, B., Schneider, A., Ramankutty, N., Sibley, A., and Huang, X. M.: MODIS Collection 5 global land cover: Algorithm refinements and characterization of new datasets, Remote Sens Environ, 114, 168-182, 10.1016/j.rse.2009.08.016, 2010.

Fritz, S., McCallum, I., Schill, C., Perger, C., See, L., Schepaschenko, D., van der Velde, M., Kraxner, F., and Obersteiner, M.: Geo-Wiki: An online platform for improving global land cover, Environ Modell Softw, 31, 110-123, http://dx.doi.org/10.1016/j.envsoft.2011.11.015, 2012.

Gorelick, N., Hancher, M., Dixon, M., Ilyushchenko, S., Thau, D., and Moore, R.: Google Earth Engine: Planetary-scale geospatial analysis for everyone, Remote Sens Environ, 202, 18-27, https://doi.org/10.1016/j.rse.2017.06.031, 2017.

Hansen, M. C., DeFries, R. S., Townshend, J. R. G., Sohlberg, R., Dimiceli, C., and Carroll, M.: Towards an operational MODIS continuous field of percent tree cover algorithm: examples using AVHRR and MODIS data, Remote Sens Environ, 83, 303-319, Pii S0034-4257(02)00079-2 Doi 10.1016/S0034-4257(02)00079-2, 2002.

415 Hansen, M. C., Potapov, P. V., Moore, R., Hancher, M., Turubanova, S. A., Tyukavina, A., Thau, D., Stehman, S. V., Goetz, S. J., Loveland, T. R., Kommareddy, A., Egorov, A., Chini, L., Justice, C. O., and Townshend, J. R.: High-resolution global maps of 21st-century forest cover change, Science, 342, 850-853. Data available on-line from: http://earthenginepartners.appspot.com/science-2013-global-forest., 10.1126/science.1244693, 2013.

Hudak, A. T., Lefsky, M. A., Cohen, W. B., and Berterretche, M.: Integration of lidar and Landsat ETM+ data for estimating and mapping forest canopy height, Remote Sens Environ, 82, 397-416, https://doi.org/10.1016/S0034-4257(02)00056-1, 2002.

420 PRODES Legal Amazon Deforestation Monitoring System: http://www.obt.inpe.br/OBT/assuntos/programas/amazonia/prodes, last

Jenkins, C. N., Pimm, S. L., and Joppa, L. N.: Global patterns of terrestrial vertebrate diversity and conservation, P Natl Acad Sci USA, 110, E2602-E2610, 10.1073/pnas.1302251110, 2013.

Leitold, V., Morton, D. C., Longo, M., dos-Santos, M. N., Keller, M., and Scaranello, M.: El Niño drought increased canopy turnover in Amazon forests, New Phytol, 219, 959-971, 10.1111/nph.15110, 2018.

425 Li, G., Lu, D., Moran, E., Calvi, M. F., Dutra, L. V., and Batistella, M.: Examining deforestation and agropasture dynamics along the Brazilian TransAmazon Highway using multitemporal Landsat imagery, Gisci Remote Sens, 56, 161-183, 10.1080/15481603.2018.1497438, 2019.

Lovejoy, T. E. and Nobre, C.: Amazon tipping point: Last chance for action, Sci Adv, 5, ARTN eaba2949 10.1126/sciadv.aba2949, 2019.

Lund, H. G.: Definitions of Forest, Deforestation, Aorestation, and Reforestation (Forest Information Services), 2014.

430 Markus, T., Neumann, T., Martino, A., Abdalati, W., Brunt, K., Csatho, B., Farrell, S., Fricker, H., Gardner, A., Harding, D., Jasinski, M., Kwok, R., Magruder, L., Lubin, D., Luthcke, S., Morison, J., Nelson, R., Neuenschwander, A., Palm, S., Popescu, S., Shum, C. K., Schutz, B. E., Smith, B., Yang, Y., and Zwally, J.: The Ice, Cloud, and land Elevation Satellite-2 (ICESat-2): Science requirements, concept, and implementation, Remote Sens Environ, 190, 260-273, https://doi.org/10.1016/j.rse.2016.12.029, 2017.

Matricardi, E. A. T., Skole, D. L., Costa, O. B., Pedlowski, M. A., Samek, J. H., and Miguel, E. P.: Long-term forest degradation surpasses
435 deforestation in the Brazilian Amazon, Science, 369, 1378-1382, 10.1126/science.abb3021, 2020.

Mitchard, E. T. A.: The tropical forest carbon cycle and climate change, Nature, 559, 527-534, 10.1038/s41586-018-0300-2, 2018.

Nepstad, D., McGrath, D., Stickler, C., Alencar, A., Azevedo, A., Swette, B., Bezerra, T., DiGiano, M., Shimada, J., da Motta, R. S., Armijo, E., Castello, L., Brando, P., Hansen, M. C., McGrath-Horn, M., Carvalho, O., and Hess, L.: Slowing Amazon deforestation through public policy and interventions in beef and soy supply chains, Science, 344, 1118-1123, 10.1126/science.1248525, 2014.

440 Ochoa-Quintero, J. M., Gardner, T. A., Rosa, I., Ferraz, S. F. D., and Sutherland, W. J.: Thresholds of species loss in Amazonian deforestation frontier landscapes, Conserv Biol, 29, 440-451, 10.1111/cobi.12446, 2015.

Olofsson, P., Stehman, S. V., Woodcock, C. E., Sulla-Menashe, D., Sibley, A. M., Newell, J. D., Friedl, M. A., and Herold, M.: A global land-cover validation data set, part I: fundamental design principles, Int J Remote Sens, 33, 5768-5788, 10.1080/01431161.2012.674230, 2012.

445 Qin, Y. and Xiao, X.: Annual PALSAR/MODIS forest and evergreen forest maps in the Brazilian Amazon, figshare [dataset], 10.6084/m9.figshare.21445590.v1, 2022a.

Qin, Y. and Xiao, X.: Codes for forest and evergreen forest mapping in the Brazilian Amazon, figshare [code], 10.6084/m9.figshare.21445626.v1, 2022b.

Qin, Y., Xiao, X., Dong, J., Zhang, G., Roy, P. S., Joshi, P. K., Gilani, H., Murthy, M. S., Jin, C., Wang, J., Zhang, Y., Chen, B., Menarguez,
450 M. A., Biradar, C. M., Bajgain, R., Li, X., Dai, S., Hou, Y., Xin, F., and Moore, B., 3rd: Mapping forests in monsoon Asia with ALOS PALSAR 50-m mosaic images and MODIS imagery in 2010, Sci Rep, 6, 20880, 10.1038/srep20880, 2016a.

Qin, Y. W., Xiao, X. M., Dong, J. W., Zhang, G. L., Shimada, M., Liu, J. Y., Li, C. G., Kou, W. L., and Moore, B.: Forest cover maps of China in 2010 from multiple approaches and data sources: PALSAR, Landsat, MODIS, FRA, and NFI, Isprs Journal of Photogrammetry and Remote Sensing, 109, 1-16, 10.1016/j.isprsjprs.2015.08.010, 2015.

455 Qin, Y. W., Xiao, X. M., Dong, J. W., Zhou, Y. T., Wang, J., Doughty, R. B., Chen, Y., Zou, Z. H., and Moore, B.: Annual dynamics of forest areas in South America during 2007-2010 at 50m spatial resolution, Remote Sens Environ, 201, 73-87, 10.1016/j.rse.2017.09.005, 2017.

Qin, Y. W., Xiao, X. M., Dong, J. W., Zhang, Y., Wu, X. C., Shimabukuro, Y., Arai, E., Biradar, C., Wang, J., Zou, Z. H., Liu, F., Shi, Z., Doughty, R., and Moore, B.: Improved estimates of forest cover and loss in the Brazilian Amazon in 2000-2017, Nature Sustainability, 2,
460 764-772, 10.1038/s41893-019-0336-9, 2019.

Qin, Y. W., Xiao, X. M., Wigneron, J. P., Ciais, P., Brandt, M., Fan, L., Li, X. J., Crowell, S., Wu, X. C., Doughty, R., Zhang, Y., Liu, F., Sitch, S., and Moore, B.: Carbon loss from forest degradation exceeds that from deforestation in the Brazilian Amazon, Nat Clim Change, 11, 442-448, 10.1038/s41558-021-01026-5, 2021.

Qin, Y. W., Xiao, X. M., Dong, J. W., Zhang, G. L., Roy, P. S., Joshi, P. K., Gilani, H., Murthy, M. S. R., Jin, C., Wang, J., Zhang, Y., Chen,
465 B. Q., Menarguez, M. A., Biradar, C. M., Bajgain, R., Li, X. P., Dai, S. Q., Hou, Y., Xin, F. F., and Moore, B.: Mapping forests in monsoon Asia with ALOS PALSAR 50-m mosaic images and MODIS imagery in 2010, Sci Rep-Uk, 6, 10.1038/srep20880, 2016b.

18

Reiche, J., Lucas, R., Mitchell, A. L., Verbesselt, J., Hoekman, D. H., Haarpaintner, J., Kellndorfer, J. M., Rosenqvist, A., Lehmann, E. A., Woodcock, C. E., Seifert, F. M., and Herold, M.: Combining satellite data for better tropical forest monitoring, Nature Clim. Change, 6, 120-122, 10.1038/nclimate2919, 2016.

470 Saatchi, S. S., Harris, N. L., Brown, S., Lefsky, M., Mitchard, E. T. A., Salas, W., Zutta, B. R., Buermann, W., Lewis, S. L., Hagen, S., Petrova, S., White, L., Silman, M., and Morel, A.: Benchmark map of forest carbon stocks in tropical regions across three continents, P Natl Acad Sci USA, 108, 9899-9904, DOI 10.1073/pnas.1019576108, 2011.

Sexton, J. O., Noojipady, P., Song, X.-P., Feng, M., Song, D.-X., Kim, D.-H., Anand, A., Huang, C., Channan, S., Pimm, S. L., and Townshend, J. R.: Conservation policy and the measurement of forests, Nat Clim Change, 6, 192-196, 10.1038/nclimate2816, 2015.

475 Shimada, M., Isoguchi, O., Tadono, T., and Isono, K.: PALSAR Radiometric and Geometric Calibration, Ieee T Geosci Remote, 47, 3915-3932, Doi 10.1109/Tgrs.2009.2023909, 2009.

Shimada, M., Itoh, T., Motooka, T., Watanabe, M., Shiraishi, T., Thapa, R., and Lucas, R.: New global forest/non-forest maps from ALOS PALSAR data (2007-2010), Remote Sens Environ, 155, 13-31, 10.1016/j.rse.2014.04.014, 2014.

Skole, D. and Tucker, C.: Tropical Deforestation and Habitat Fragmentation in the Amazon - Satellite Data from 1978 to 1988, Science, 260, 480 1905-1910, DOI 10.1126/science.260.5116.1905, 1993.

Sonter, L. J., Herrera, D., Barrett, D. J., Galford, G. L., Moran, C. J., and Soares-Filho, B. S.: Mining drives extensive deforestation in the Brazilian Amazon, Nature Communications, 8, 1013, 10.1038/s41467-017-00557-w, 2017.

Souza, C. M., Z. Shimbo, J., Rosa, M. R., Parente, L. L., A. Alencar, A., Rudorff, B. F. T., Hasenack, H., Matsumoto, M., G. Ferreira, L., Souza-Filho, P. W. M., de Oliveira, S. W., Rocha, W. F., Fonseca, A. V., Marques, C. B., Diniz, C. G., Costa, D., Monteiro, D., Rosa, E. R., 485 Vélez-Martin, E., Weber, E. J., Lenti, F. E. B., Paternost, F. F., Pareyn, F. G. C., Siqueira, J. V., Viera, J. L., Neto, L. C. F., Saraiva, M. M., Sales, M. H., Salgado, M. P. G., Vasconcelos, R., Galano, S., Mesquita, V. V., and Azevedo, T.: Reconstructing Three Decades of Land Use and Land Cover Changes in Brazilian Biomes with Landsat Archive and Earth Engine, Remote Sens-Basel, 12, 2735, 2020.

Stehman, S. V., Olofsson, P., Woodcock, C. E., Herold, M., and Friedl, M. A.: A global land-cover validation data set, II: augmenting a stratified sampling design to estimate accuracy by region and land-cover class, Int J Remote Sens, 33, 6975-6993, 490 10.1080/01431161.2012.695092, 2012.

Tang, H., Armston, J., Hancock, S., Marselis, S., Goetz, S., and Dubayah, R.: Characterizing global forest canopy cover distribution using spaceborne lidar, Remote Sens Environ, 231, 111262, https://doi.org/10.1016/j.rse.2019.111262, 2019a.

Tang, H., Song, X.-P., Zhao, F. A., Strahler, A. H., Schaaf, C. L., Goetz, S., Huang, C., Hansen, M. C., and Dubayah, R.: Definition and measurement of tree cover: A comparative analysis of field-, lidar- and landsat-based tree cover estimations in the Sierra national forests, 495 USA, Agr Forest Meteorol, 268, 258-268, https://doi.org/10.1016/j.agrformet.2019.01.024, 2019b.

Thapa, R. B., Itoh, T., Shimada, M., Watanabe, M., Takeshi, M., and Shiraishi, T.: Evaluation of ALOS PALSAR sensitivity for characterizing natural forest cover in wider tropical areas, Remote Sens Environ, 155, 32-41, DOI 10.1016/j.rse.2013.04.025, 2014.

Tyukavina, A., Hansen, M. C., Potapov, P. V., Stehman, S. V., Smith-Rodriguez, K., Okpa, C., and Aguilar, R.: Types and rates of forest disturbance in Brazilian Legal Amazon, 2000-2013, Sci Adv, 3, e1601047, 10.1126/sciadv.1601047, 2017.

500 UNFAO: Expert Meeting on Harmonizing Forest-Related Definitions for Use by Various Stakeholders, 2002.

Woodcock, C. E., Allen, R., Anderson, M., Belward, A., Bindschadler, R., Cohen, W., Gao, F., Goward, S. N., Helder, D., Helmer, E., Nemani, R., Oreopoulos, L., Schott, J., Thenkabail, P. S., Vermote, E. F., Vogelmann, J., Wulder, M. A., Wynne, R., and Team, L. S.: Free access to Landsat imagery, Science, 320, 1011-1011, 2008.

Xiao, X., Dorovskoy, P., Biradar, C., and Bridge, E.: A library of georeferenced photos from the field, Eos, Transactions American 505 Geophysical Union, 92, 453-454, 10.1029/2011eo490002, 2011.

Xiao, X., Boles, S., Frolking, S., Salas, W., Moore, B., Li, C., He, L., and Zhao, R.: Observation of flooding and rice transplanting of paddy rice fields at the site to landscape scales in China using VEGETATION sensor data, Int J Remote Sens, 23, 3009-3022, 10.1080/01431160110107734, 2002.

Xiao, X. M., Biradar, C. M., Czarnecki, C., Alabi, T., and Keller, M.: A Simple Algorithm for Large-Scale Mapping of Evergreen Forests 510 in Tropical America, Africa and Asia, Remote Sens-Basel, 1, 355-374, Doi 10.3390/Rs1030355, 2009.